INTERNATIONAL JOURNAL OF RESEARCH IN AERONAUTICAL AND MECHANICAL ENGINEERING
WWW.IJRAME.COM
ISSN (ONLINE): 2321-3051

Vol.7 Issue 7, July 2019 Pg: -01-14

Effect of Cumulative stress in jet engine blade due to bird strike impact at high altitude

Mihir Shah[1], Darshil Soni[2], Kashyap Sutariya[3], Yash Varma[4]

[1,2,3,4]*student*, Mechanical Engineering Department, A. D. Patel Institute of Technology, P.O. Box No.52 Vitthal Udyognagar, New Vallabh Vidyanagar-388212, Anand, Gujarat, India

mihirshah3107@gmail.com[1], sonidarshil15@gmail.com[2], sutariyakashyap95@gmail.com[3], yashvarma181@gmail.com[4]

Abstract

High stresses are induced in the blade of jet engine during flight condition, which are significant threat to the flight safety and have caused a number of accidents with human casualties. Bird strike, fatigue, creep, stagnation pressure and centrifugal force etc. are the factors that can cause damage to the blade. It is found from literature that centrifugal forces lead to rise in stresses at root section during flight condition. In such situation, bird strike has significant impact for damage of the blade. In this paper, simulation of jet engine blades at 810 rad/sec (7734 RPM) with bird strike velocity of 89.611 m/s (174.18 Knot) was considered. Initially, simulation of single blade was carried out using pressure and stress distribution at high altitude by fluid structural interaction. Effective stress versus time graph was plotted to understand the physical phenomenon through simulation so that required modification in single blade design can be thought to avoid accidents.

Keywords: LS-DYNA, Bird-strike, CE\SE solver, Pressure distribution, Centrifugal stress.

1. Introduction

Jet engine blades are subjected to stresses due to centrifugal force and air flow pressure during normal flight conditions. The jet engine blades are subjected to very strenuous environments like high temperatures, high stresses, and a potentially high vibration environment. All three of these factors can lead to blade failures, which can destroy the engine as reported in (L K Gupta et al., 2013). Intense stresses are induced on the blade in an event of bird strike. From 1990 to 2008 almost 90,000 bird strikes on commercial aircraft have been reported to the Federal Aviation Administration (FAA) solely in the USA (Dolbeer RA et al., 2009), leading to immense monetary losses due to repair, delay and cancellations. Annual cost values from 614 million to 1.28 billion US$ as reported in (Allan JR et al., 2001). Many researchers have presented independent simulation of stresses in a blade arising due to centrifugal forces, air flow pressure, and bird strike (Aaron J Siddens et al.,

2013) (Miyachi et al., 1991). The project aimed to investigate cumulative effect of the loads on the blade. The problem was multidisciplinary and involved non-linear simulation in complex domains using advanced techniques. A detailed finite element model of the jet engine turbine was adapted and customized in LS-DYNA software. The CE\SE (Conservation Element\Solution Element) solver initially imparts the pressure by simulating air flow on the blades. The pressure distribution was found in good agreement with the results available in the literature (Karna S Patel et al., 2014) as shown in figure 4(a). The centrifugal force was induced in the blades as a result of rotation (810 rad/sec) of the turbine. At the same time, a foreign object like bird drawn into the engine due to air flow, which damages the blade, outer casing and other components.

A bird model was developed and validated against available experimental results reported in literature. The bird is generated using SPH (Smoothed Particle Hydrodynamics) method. The bird was made to impact on the blades at a velocity of 174.18 knot (89.611 m/s). The obtained results show cumulative effect of different types of loads on the engine blades, which shall be useful in design and optimization of an engine blade.

Although, aerospace organizations have conducted numerous in-house bird strike, effect of centrifugal force, blade life-cycle experiments at earth ground level but it is difficult to perform these experiments for real flight conditions. This paper emphasis on determination of combine stresses on the blades, in which the engine is kept in the artificially generated real time flight boundary conditions.

2. Experimental Method

Following assumptions are considered for the simulation of jet blades for bird strikes:

- Angular velocity of blade - 810 rad/sec.
- Material is homogeneous
- Mass of bird - 4 lb.(1.8kg) (Chuan KC, 2006)
- Impact velocity of bird on the blades – 174.18 knots (89.611 m/s).
- Velocity of air is uniform with specific range of altitude

2.1 Phases of flight

Three phases of flight like take –off, climb and cruise at different altitude with other input conditions like pressure, temperature, density and air velocity are simulated for stress determination using LS DYNA. The different phases of flight are:

Take-off/Landing Velocity: - (120-150) Knots

Climb velocity: - (280-310) Knots

Cruise Velocity: - (240-250) Knots

Output measures are stagnation pressure acting on fluid, Von-misses stress and external pressure acting on blade.

INTERNATIONAL JOURNAL OF RESEARCH IN AERONAUTICAL AND MECHANICAL ENGINEERING
WWW.IJRAME.COM
ISSN (ONLINE): 2321-3051

Vol.7 Issue 7,
July 2019
Pg: -01-14

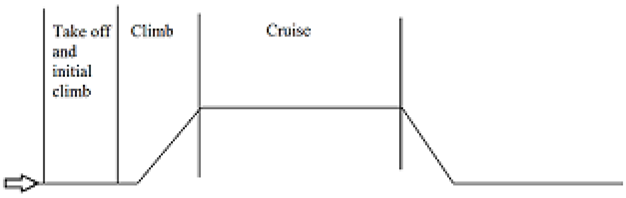

Figure 1: Phases of flight.

2.2 Material and dimensions of blade

Titanium fan blades have historically shown good performance due to the metal's unique combination of mechanical, corrosion and physical properties. Titanium has excellent tensile and yield strength, low life cycle cost, readily available, ease in fabrication combined with its low-density results in the highest strength to weight ratio compared to other structural metals. The initially higher cost of titanium can be regained several-fold by savings resulting from longer component life and corresponding reduction in equipment maintenance and aircraft downtime. Moreover, titanium creates an oxide layer on the surface of the blade, which can resist interaction with other atmospheric elements (Leye M.Amoo, 2013).

T. Miyachi discussed that application of polymer matrix composite materials for fan blades is highly effective to reduce the weight of high turbo-fan engines. The weight of the fan would be reduced by 30% or more (T. Miyachi, 1989) using composite materials such as Ti 6Al- 4V. The properties of material are as shown in Table-1, which was considered in simulation.

Figure 2 shows single blade structure with dimensions as per Table-2. The developed model of single blade was used for simulation. The model of the blade was obtained from aerospace working group of LSTC.

Table 1: Properties of material

Parameter	**Notation**	**Ti 6Al- 4V**	**SI Unit**
Density	ρ	0.160043 (lb./in^3)	4429.97 (Kg/m^3)
Poisson ratio	Y	0.33	
Modulus of elasticity	E	1.6E+7 (psi)	1.1E+11 (N/m^3)
Static yield limit	A	159,246 (psi)	1.09E+9 (N/m^3)
Strain hardening modulus	B	158,376	

IJRAME

INTERNATIONAL JOURNAL OF RESEARCH IN AERONAUTICAL AND MECHANICAL ENGINEERING
WWW.IJRAME.COM
ISSN (ONLINE): 2321-3051

Vol.7 Issue 7, July 2019
Pg: -01-14

Table 2: Feature of blade

Component	Measures	SI Units
Blade-tip radius	20 in	0.508 m
Blade-root radius	6 in	0.152 m
Blade-root area	0.9 in.^{2}	0.0005 m^2
Blade-root stagger angle	17^o	-
Blade-tip stagger angle	40^o	-
Blade chord at tip	5.2 in	0.132 m
Blade chord at root	4.5 in	0.114 m

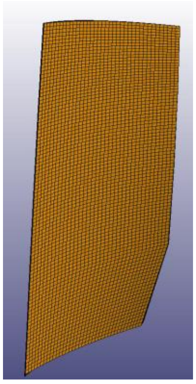

Figure 2: Structure of blade used for simulation

2.3 Pressure and stress distribution because of air flow in a blade

The pressure acting on the blades because of the air flow is different at different atmospheric conditions. For this varying condition, the CESE solver (compressible fluid solver) is used in LS-DYNA. The blade is kept in the rectangular shell type box as shown in figure 3. The air flow behaviour and parameters of CESE solver are specified in Table 3(a)-3(b).

CESE_EOS_IDEAL_GAS define the coefficients C_v and C_p in the equation of state for an ideal gas in CESE fluid solver. CESE_MAT_001 (GAS) defines the fluid (gas) properties in a viscous flow for the CESE solver.

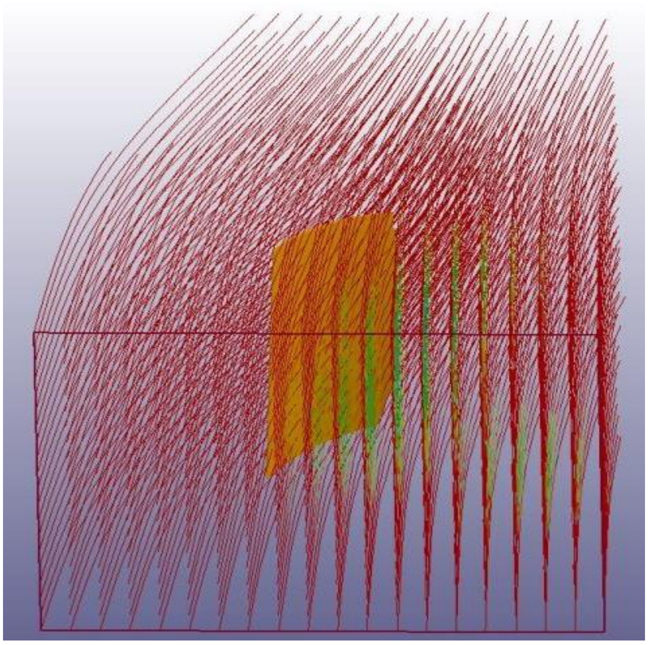

Figure 3: Streamline of air impacting on blade

Table 3(a): Different keywords used in CESE solver

Sr. No.	Keywords	Purpose
1	CESE_BOUNDARY_NON _REFLECTIVE	To develop non-disturbed uniform flow for specified boundary at entry (Input) level.
2	CESE_EOS_IDEAL_GAS	To define coefficients C_v and C_p in the equation of state for an ideal gas.
3	CESE_MAT_001 (GAS)	To define the fluid (gas) properties.

Table 3(b): Data of air properties at different altitude

Sr. No.	Altitude (ft.)	Velocity (v) of air	Pressure of air(psi)
1	30-900ft	65m/s	14.679 psi
2	1000-9000 ft.	108m/s	13.669 psi

IJRAME
INTERNATIONAL JOURNAL OF RESEARCH IN AERONAUTICAL AND MECHANICAL ENGINEERING
WWW.IJRAME.COM
ISSN (ONLINE): 2321-3051
Vol.7 Issue 7, July 2019
Pg: -01-14

3	Above 10,000 ft.	150 m/s	10.669 psi

Value of air density and pressure is obtained from International Atmosphere Standard [8]. The value of air velocity can be calculated by the following Bernoulli's equation.

$P= ½ \rho v_a^2$

Where, P = Pressure of Air, ρ = Density and v_a = Air Velocity

For different altitude condition, the values of pressure and stress are mentioned in table 3(c).

This case is performed to obtain the trend of maximum stress level at different altitudes in the stationary blade by neglecting effect of bird strike and centrifugal force. It is observed that with increase in the altitude the trend of stress and pressure is dwindled.

Table 3(c): Max pressure & stress at different altitude

Sr. No.	Altitude (ft.)	Max. Pressure(psi)	Max. Stress(psi)
1	30-900ft	23.186	27.3096
2	1000-9000 ft.	21.5759	25.4097
3	Above 10,000 ft.	15.9422	18.7717

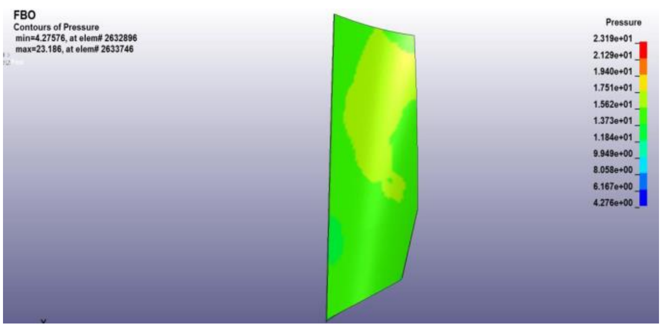

Figure 4(a): Pressure on the blade, when fluid strike on the blade

INTERNATIONAL JOURNAL OF RESEARCH IN AERONAUTICAL AND MECHANICAL ENGINEERING
WWW.IJRAME.COM
ISSN (ONLINE): 2321-3051

Vol.7 Issue 7,
July 2019
Pg: -01-14

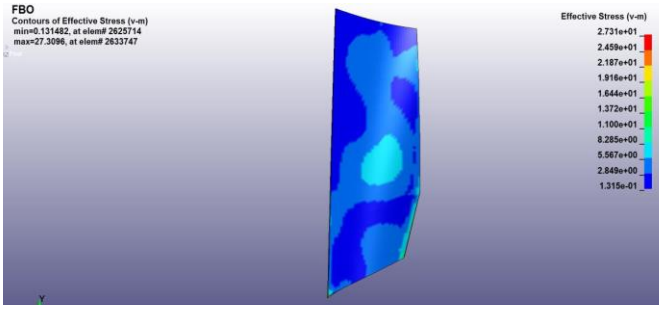

Figure 4(b): Stress on the blade, when fluid strike on the blade

2.4 Centrifugal stress generated in blade

The blades as shown in Figure 5(a) are rotating with angular velocity of 816 rad/sec. Using VELOCITY_GENERATION value is assigned to the part id of the blades. Approximate 101827psi [702.07 MPa] of stress was induced in the a particular element of the blade, where bird may collide with blade. Average 6.110E+04psi [421Mpa] of stress on the blade is developed as shown in figure 5(a). The stress near hub section are higher than tip section as shown in figure 5(b). Effective stress Vs time graph of different nodes near bird strike loacations is plotted as shown in figure 6.

The centrifugal force in a high speed rotating blade can not be ignored because centrifugal acceleration due to rotation of fan reaches over 50000 times of gravitational acceleration. Because of that impact resistance increased and deformation of the blade is reduced **[**5**].**

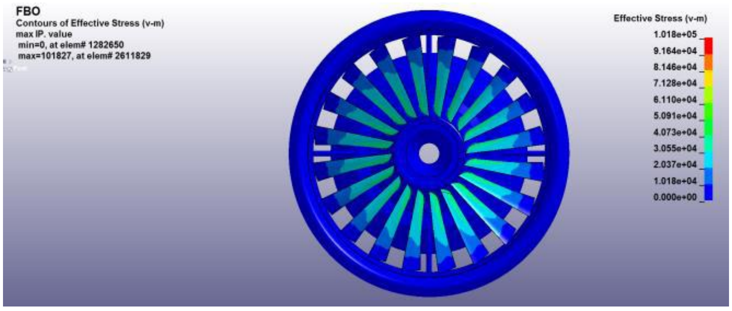

Figure 5(a): Variation of stress from hub to tip of blade

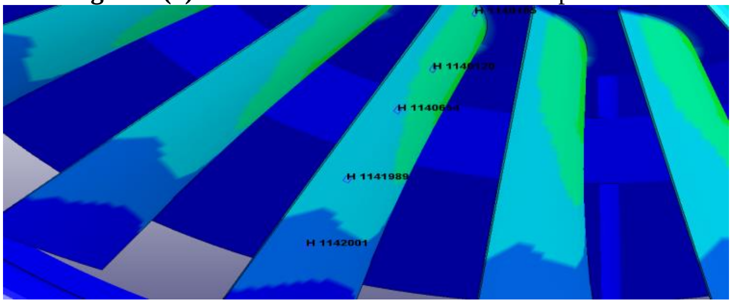

Figure 5(b): Variation of stress from hub to tip of blade

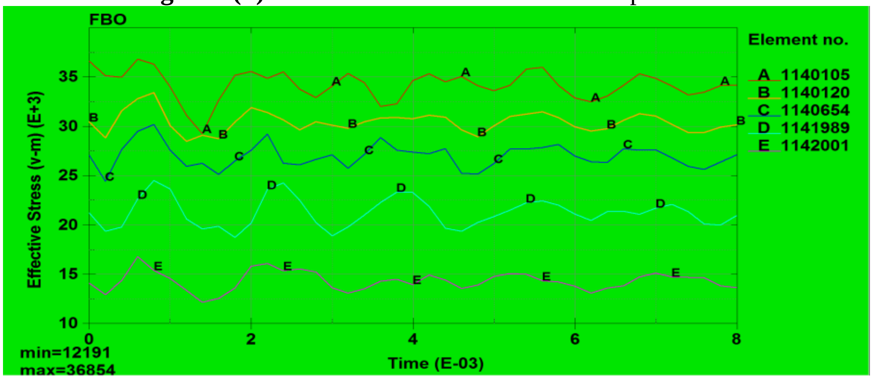

Figure 6: Graph of stress v/s time

2.5 Stress in a blade due to bird strike

Separate test for the bird strike is done on the solid single blade. The Smoothed Particle Hydrodynamics (SPH) was first introduced in the field of astrophysics to deal with fluid masses moving arbitrarily in three-dimensional space. Since, the SPH method is a purely Lagrangian technique, it can be easily linked to finite element solutions based on the Lagrangian formulation. In addition, due to the absence of a mesh connecting the individual particles, the SPH technique can handle problems involving large deformations with greater ease. In the SPH method, the continuum is treated as a random set of particles that interact with each other. SPH is a technique that has foundations in the interpolation theory, and allows any function to be expressed in terms of the values of the same function at a set of disordered points that makeup the continuum. Spatial derivatives of various field variables are computed using kernel estimates, in the absence of regular connectivity between the particles found in methods that use a mesh (Nizampatnam et al., 2007)**.** The shape of the bird is considered to be the sphere with density 950 kg/m^3.

According to Martin NF, the projectile response during an impact can be divided into five categories as a function of the impact velocity: elastic, plastic, hydrodynamic, sonic or explosive. During an elastic impact, the internal stresses in the projectile are below the material strength so that it will rebound. With increasing impact velocity, plastic response of the impactor begins but the material strength is still sufficient to prevent a fluid-like behaviour. A further increase of impact velocity causes internal stresses to exceed the projectile's strength and fluid-like flow occurs. At this impact velocity, the material density determines the response of the impactor. Material strength will not play a role in this case. This flow behavior of real birds can typically be observed in high-speed films of impact tests.

Therefore, the bird impactor is treated as a so-called 'soft body' at the velocities of interest, since the stresses that develop within the bird are significantly higher than its own strength. The load is spread over a relatively large area during the impact (Martin NF, 1990). Collisions between engines and birds during flight are classified as soft impact events. Soft impact occurs when the projectile has a much lower strength than the

IJRAME

INTERNATIONAL JOURNAL OF RESEARCH IN AERONAUTICAL AND MECHANICAL ENGINEERING
WWW.IJRAME.COM
ISSN (ONLINE): 2321-3051

Vol.7 Issue 7,
July 2019
Pg: -01-14

target, causing extensive deformation of the projectile over the target surface (Kim et al., 2010) (Wilbeck and J.S., 1981).

A fluid material model coupled with a pressure-volume equation of state (EOS) was used to define the bird's behaviour. This combined model defined the bird mass and related the volume change of an SPH particle to the hydrostatic pressure over the particle, while ignoring deviatoric stresses from shear stiffness (a common technique for modelling fluids) (Jenq et al., 2007).

Stress distribution due to bird strike and effective stress vs time is depicted in figure 7 and 8 respectively. From the performed simulation, It was observed that 44778 psi (308.73 MPa) of effective stress on the blade for only bird strike consideration. The results are very much validated with other references. The middle portion of Blade begins to be impacted by the bird. The maximum equivalent stress in the contacting area is 265 MPa (Guan Yupu et al., 2008).

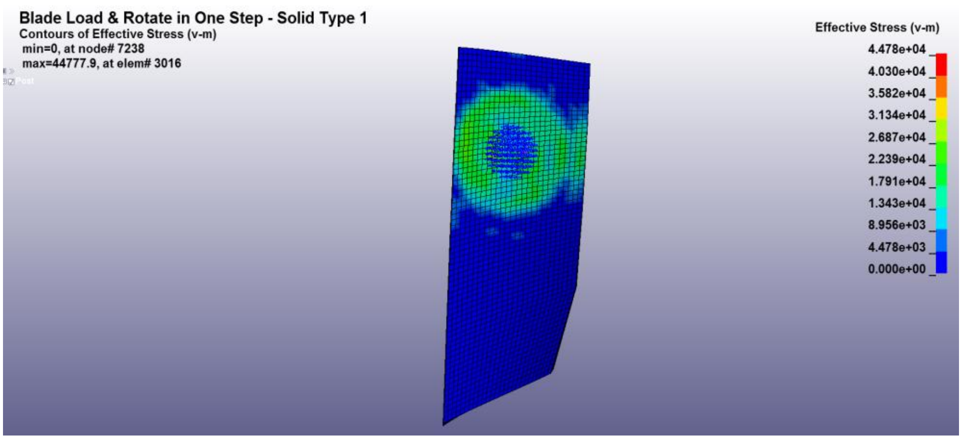

Figure 7: Stress generated on the blade at a time of bird-strike

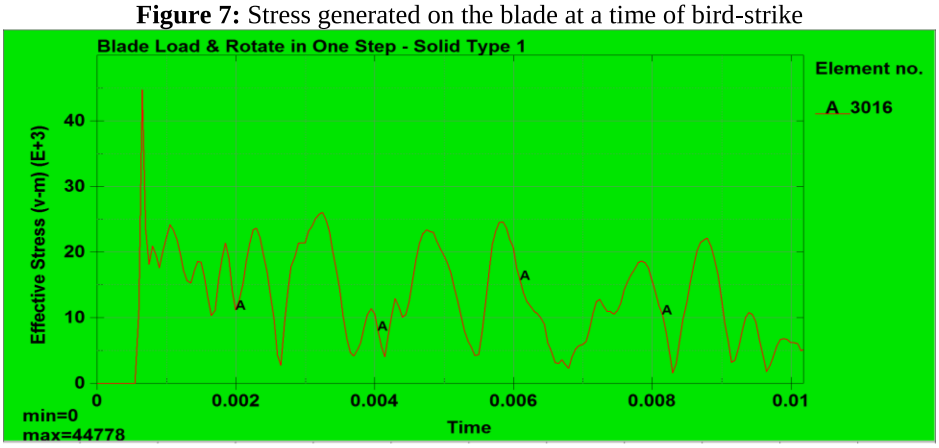

Figure 8: Graph of stress v/s time

2.6 Cumulative stress determination in a blade

Investigation of combine stresses is also carried out, considering all the previous conditions to mimic real scenario of flight. To determine the stresses because of centrifugal force the angular velocity is assign to blade rotor is 810 rad/sec.

LS-Dyna consists of the two post: multi-solver post and basic post. The multi-solver post gives results related to fluid dynamics while the basic post give result related to the solid/shell structure. However, the streamlines of the fluid are not generated in the basic post result of the bird-strike that can be availed using multi post solver.

The figure 9 represents the pressure of the fluid. The pressure gets reduced from 1.944E+01psi to 1.758E+01psi, when it strikes to the blade. [The multi-solver post is not allowing to visible the structure to structure interaction but it considers the effect of the interaction.] The figure 10 indicates pressure value on the fringe level of blades.

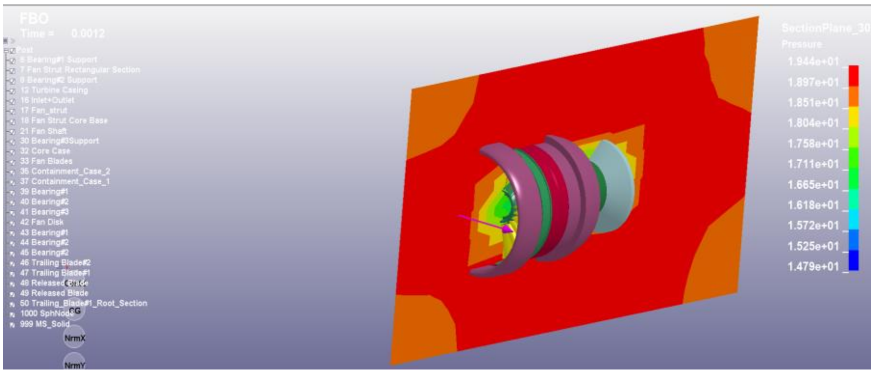

Figure 9: Pressure of the fluid. When strike on the rotating blade

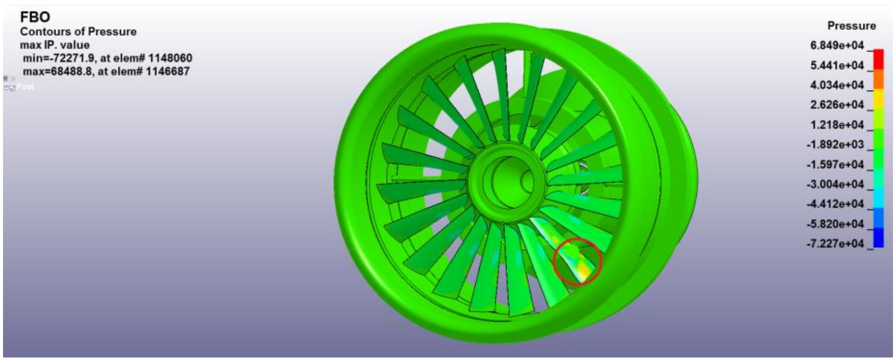

Figure 10: Pressure promoted on the blade due to bird strike

Pressure generated due to the air over the engine is about 1.218E+04 psi which surges to 2.626E+04 psi at time of bird strike in targeted blade. Other parts like casing and shaft were defined rigid to minimize simulation time. Hence, no stress is acting on them. Stress variation in the blades is caused by all above mentioned conditions. The above results show the stress distribution on the blade at altitude 30-900ft. During the bird strike, large amount of stress was generated at the root section and the area where impact take place. Hence, particular elements were selected and the graph has been plotted as shown in Fig.13.

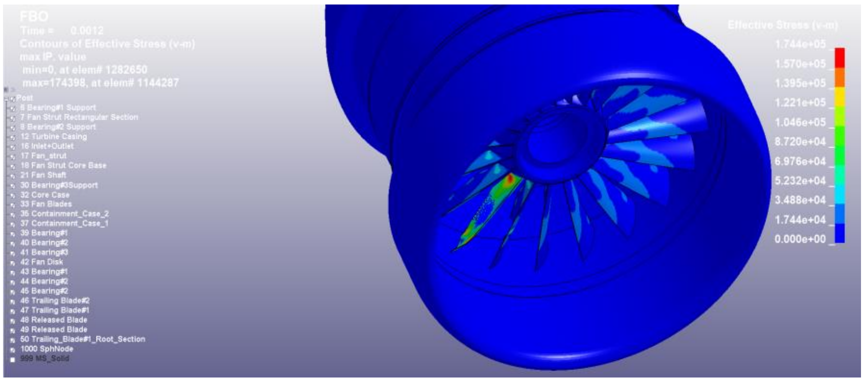

Figure 11: High stresses are promoted in the blade due to bird strike

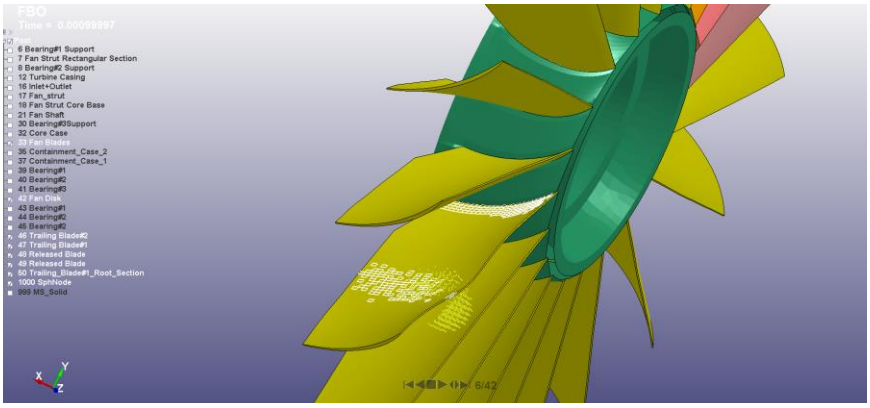

Figure 12: Selected element of the targeted blade

IJRAME

INTERNATIONAL JOURNAL OF RESEARCH IN AERONAUTICAL AND MECHANICAL ENGINEERING
WWW.IJRAME.COM
ISSN (ONLINE): 2321-3051

Vol.7 Issue 7, July 2019 Pg: -01-14

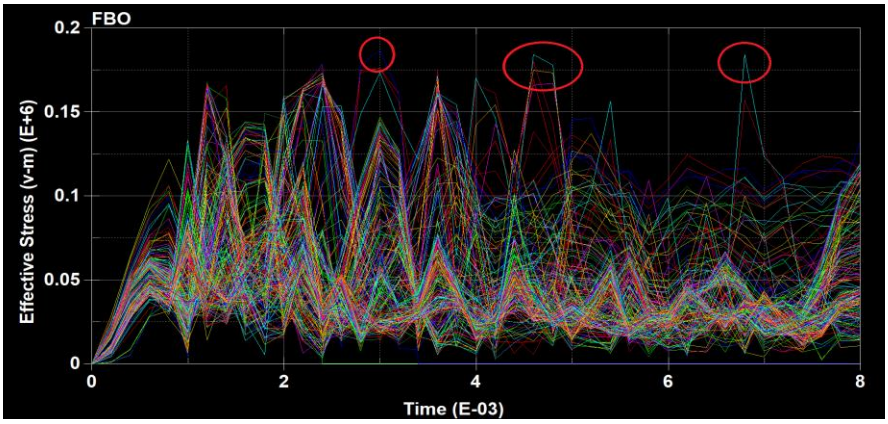

Figure 13: Graph of Stress V/s Time

At time of bird strike, about 174389 psi [1202.36 MPa] stresses are induced, after that some of the element experienced lofty trend in the stress due to bending which cause after impact. Overall, stress of 1202.36 MPa was generated in blade throughout the event. Similarly, the results are obtained for different altitudes as presented in Table-4.

Table 4: Von-Mises stresses induced in blade at different altitude

Sr.no	Altitude range	Von-Mises Stress
1	30-900ft.	174389 psi [1202.36 MPa]
2	1000-9000ft.	173790psi [1198.23 MPa]
3	above 10,000	173477 psi [1196.08 MPa]

3. Result and discussion

The stresses at three different altitudes are found to be nearby each other (Table.4). Because at 65m/s at altitude 30-900 ft. the relative velocity is low but the density of fluid is high and increase in density tends to increase in stress and vice versa (N.A. Fleck and R.A.Smith, 1981).

For altitude above 10,000 ft. at 150m/s, the relative velocity is high but the density of fluid is low. Because of that the stress induced is nearby in each phase of flight.

4. Conclusion

Various stresses acting on jet engine blade at the different altitude is successfully obtained with the help of 'LS-Dyna' software. With its strong damage and failure modelling capabilities for transient dynamic analysis of highly nonlinear problems, LS-Dyna is an ideal tool for high speed impact situation.

Large amount of money can be saved with numerical simulations before actual testing. The numerical simulation provides more results than experiments and can be exploited to verify and complement experiment results.

By simulation results in the cumulative stress effect, the generated stress by air flow is very less compared to impact and centrifugal stress.

The impacting damage of blades caused by the bird impact on the tip of blades is more severe than that on the middle of blades.

At different altitude, the generated stresses are not changing drastically because increase in relative velocity at higher altitude have decrease in density.

By centrifugal force, the impact resistance of blades is increased and generated stress lies below the yield strength of blade material which suggests that design is safe and not cause blade failure.

References

1] Bhagi, L K Gupta, Pardeep and Vikas Rastogi *"A Brief Review on Failure of Turbine Blades"* STME-2013, Smart Technologies for Mechanical Engineering 25-26 Oct 2013 at Delhi Technological University, Delhi.

2] Dolbeer RA, Wright SE, Weller J, Begier MJ. "*Wildlife strikes to civil aircraft in The United States 1990–2008"*. FAA National Wildlife Strike Database, Serial Report Number 15, September, 2009.

3] Allan JR, Orosz AP. "*The costs of bird strikes to commercial aviation"*. In Proceedings of the 2001 bird strike committee-USA/Canada 3rd joint annual meeting, Calgary, Canada; 2001 p.*218-226*

4] Aaron J. Siddens and Javid Bayandor "*Crashworthiness for Aerospace Structures and Hybrids (CRASH),"* *Computer and Structures* Vol.122, June 2013, p.*178-191*.

5] Miyachi, T., Okumura, H., and Ohtake, K., "*An Analysis of the Effect of Centrifugal Force on the Impact Resistance of Composite Fan Blades for Turbo-Fan Engines*," SAE Technical Paper 912047, 1991p.*246-253*

6] Karna S. Patel, Saumil B. Patel, Utsav B. Patel, Prof. Ankit P. Ahuja., "*CFD Analysis of an Aerofoil",* International Journal of Engineering Research Vol.3,March 2014, p. *154-158.*

7] Chuan KC (2006) Finite element analysis of bird strikes on composite and glass panels. PhD dissertation, BSc thesis, National University of Singapore.

8] Standard Atmospheric Pressure at Different Altitudes.

9] Phases of flight- https://www.fp7-restarts.eu

10] Leye M.Amoo., "*On the design and structural analysis of jet engine fan blade structures*", Progress in Aerospace Sciences, Volume 60,2013 p. *1-11*.

11] T. Miyachi, *"Research on the Application of Composites for High Bypass Ratio Turbo-Fan Engines"*, Proceedings of the 29th Conference on Aircraft Engines, Feb. 1989, p.*20-25*.

12] LS-DYNA Aerospace Working Group.

13] LSTC-Manual Theory –III MULTI-PHYSICS-SOLVER.

14] LSTC-Manual Theory –II Material Models.

15] Nizampatnam, L. S., "Models and Methods for Bird Strike Load Predictions", PhD thesis, Wichita State University, 2007.

16] Martin NF. *"Nonlinear finite-element analysis to predict fan-blade damage due to soft-body impact"*. J Propul Power 1990, p.*445–50*.

17] Kim, M., Zammit, A. and Bayandor, J. "*Bird Strike Damage Tolerance Analysis of Composite Turbofan Engines*," 27th Congress of the International Council of the Aeronautical Sciences, Proceedings of ICAS 2010, Nice, France, 2010, p. *19-24*.

18] Wilbeck, J. S. "*Development of a Substitute Bird Model*," Journal of engineering for power Vol. 103, No. 4, 1981, pp. *725-730*.

19] Jenq, S. T., Hsiao, F. B., Lin, I. C., Zimcik, D. G. and Ensan, M. N. "*Simulation of a rigid plate hit by a cylindrical hemi-spherical tip-ended soft impactor*," Computational Materials Science Vol. 39, 2007.

20] Guan Yupu, Zhao Zhenhua, Chen Wei, Gao Deping. "*Foreign object damage to fan rotor blades of aero engine part ii: numerical simulation of bird impact*", Chinese journal of Aeronautics, Vol 21, Issue 4, August 2008, p. *328-334*

21] N.A. Fleck and R.A.Smith, "*Effect of density on tensile strength, fracture, toughness, and fatigue crack propagation behavior of sintered steel*", Taylor & Francis Vol 24, 1981, p.*121-125*.